Muscular Effort for the Characterization of Human Postural Behaviors

Emel Demircan*, Akihiko Murai, Oussama Khatib, and Yoshihiko Nakamura

Department of Mechano-Informatics, The University of Tokyo, Japan
Department of Computer Science, Stanford University, USA

Abstract. The human selection of specific postures among the infinity of possibilities is the result of a long and complex process of learning. Through learning, humans seem to come to discover the properties of their bodies and how best to put them to use when performing a task. Exploiting the body's kinematic characteristics, humans effectively use the body's mechanical advantage to improve the transmission of the muscles' tension into the forces the task requires. However, the efficiency of this transmission is also affected by the human muscle actuation physiology and dynamics. By also adjusting the body configurations to maximize this transmission of muscle tensions to resulting task forces, humans are in fact exploiting what can be termed the physiomechanical advantage of their musculoskeletal system. Here, we investigate the physiomechanical advantage of humans through several experimental validations. Based on the results of the analysis, we conclude that in learned tasks the optimization of the physiomechanical advantage corresponds to the overall minimization of the human muscular effort. The approach presented here can be applied for the motion control of human musculoskeletal models where the control is task-driven and the task consistent postures are driven by the muscular criteria.

Keywords: muscular effort, motion analysis, postural behaviors

1 Introduction

1.1 Related Work

The ability of humans to move and coordinate their limbs in the performance of common tasks is remarkable. When holding a heavy object or applying a force to the environment through a tool, the arms and body of a skillful human are configured in the most effective fashion for the task. Mathematical models have proven to be valuable tools for motor control prediction [1, 2] and for predicting the kinematically redundant body motion [3]. These models frequently characterize some element of musculoskeletal effort. Robotics-based effort models [4]

* Corresponding author at: Department of Mechano-Informatics, Faculty of Engineering, 2nd bldg., Room 82D1, The University of Tokyo, Japan, Tel: +81-3-5841-6381, E-mail: emeld@stanford.edu (E. Demircan).

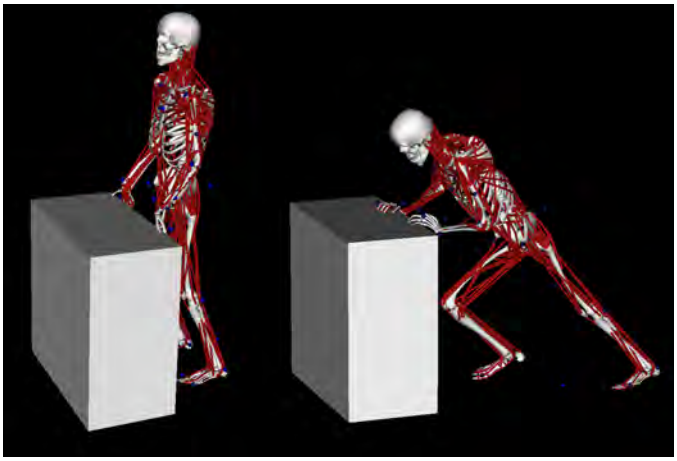

Fig. 1. The hypothesis is that in learned tasks humans minimize a criterion associated with the muscular effort. In order to push a heavy object, a human tries to best position his body to maximize the *physiomechanical advantage*.

frequently utilize quantities that are derivable purely from skeletal kinematics and that are not specific to muscle actuation and dynamics. It is thus useful to consider an analogous measure that encodes information about the overall musculoskeletal system to account for muscle actuation and its redundancy. Activation, which represents the normalized exertion of muscles, provides a natural starting point for constructing such a measure. The magnitude of muscle activation vector has been used as an optimization criterion in both static and dynamic optimizations [5].

1.2 Motivation

Recently, our effort on human motion analysis have resulted in the robotics-based synthesis of human motion [6]. Our hypothesis is that by exploiting the body's kinematic characteristics, humans effectively use the body's mechanical advantage to improve the transmission of the muscles' tension into the forces the task requires. However, the efficiency of this transmission is also affected by the human muscle actuation physiology and dynamics. By also adjusting the body configurations to maximize this transmission of muscle tensions to resulting task forces, humans are in fact exploiting what can be termed the physiomechanical advantage of their musculoskeletal system. Here, we investigate the physiomechanical advantage of human postural behaviors through several experimental validations. We speculate that in learned tasks the optimization of the physiomechanical advantage corresponds simply to the overall minimization of the human muscular effort. By validating this criteria through natural human motions, we aim at using it for the real-time posture control of human and humanoid models.

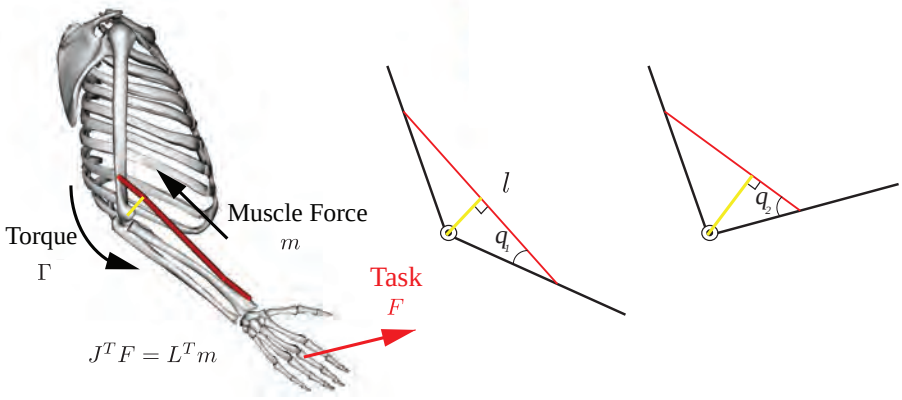

Fig. 2. Muscle/Task Relationship: The muscle-induced joint torques, Γ, are dependent on the force production, m, as well as the moment arm of the muscle, defined as the perpendicular distance (yellow line) from point of force application to the axis of rotation. Different skeletal configurations (i.e., q_1 and q_2) would result in different muscle Jacobians, $L(q)$ (Figure adapted from [7]).

2 Muscular Effort Criteria

Robotics-based effort models frequently utilize quantities that are derivable purely from skeletal kinematics and that are not specific to muscle actuation and dynamics. It is thus useful to consider an analogous measure that encodes information about the overall musculoskeletal system to account for muscle actuation and its redundancy. Since human motions are frequently linked by physiological capacities, the use of a model-based characterization of muscle systems that accounts for muscle kinematic and strength properties is critical to simulating human motion. A strategy that employs mechanical advantage to produce a posture and task force corresponds to a minimization of muscular effort (Fig. 1). While in static poses, the muscles produce joint torques to act against the gravitational torques, in dynamic skills, inertial forces are part of the effort and are taken into account accordingly.

2.1 Muscular Effort Formulation

Musculoskeletal kinematics provide us the basics for understanding the effect of the musculoskeletal geometry on muscle function and for establishing the relationship between muscle forces and resulting joint moments. Here, we define the muscle Jacobian of humen musculoskeletel system and present the muscle/task relationship for task-oriented characterization of human motion. For a human musculoskeletal system of n degrees of freedom and r muscles, a set of muscle forces, m, arises based on muscle activations, a, as well as the skeletal configuration, q and $\dot{q}$. In this model, all musculo-tendon lengths, l, can be uniquely

determined from the joint angle, q, and differential changes, dl, are given by:

$$dl = L(q)dq. \tag{1}$$

Here, L is the muscle Jacobian representing the muscle moment arms (Fig. 2). The muscle-induced joint torques, Γ, can be given using the muscle forces, m, and the task forces, F, by the relationship:

$$\Gamma = J^T(q)F = L^T(q)m. \tag{2}$$

In order to investigate the muscular effort in terms of the musculoskeletal parameters, we introduce the function, $\Phi(q)$, to represent the physiomechanics of the human musculoskeletal system including the Jacobian, $J(q)$, the muscle Jacobian, $L(q)$, and the muscle force-generating capacity, C (i.e., peak isometric forces). The physiomechanical advantage function, $\Phi(q)$, is defined as:

$$\Phi = J(q)(L^T(q)C^2L(q))^{-1}J^T(q), \tag{3}$$

and captures the spacial characterization of the muscular effort measure by connecting the muscle physiology to the resulting task through the Jacobian.

Using the physiomechanical advantage function, $\Phi(q)$, for task-based effort criteria, and the generalized operational space forces, F, for the resulting task requirements, the overall effort function can be written in the form:

$$E = F^T\Phi(q)F. \tag{4}$$

2.2 Dynamic Consistency with Contacts

For k contacts with the environment, we form the contact Jacobian by concatenating all the Jacobians for each contact:

$$J_c(q) = \begin{bmatrix} J_{c_1} \\ J_{c_2} \\ \cdot \\ \cdot \\ \cdot \\ J_{c_k} \end{bmatrix}. \tag{5}$$

Similarly, for m tasks to be performed by the musculoskeletal system, we form the task Jacobian by concatenating all the Jacobians for each task:

$$J_t(q) = \begin{bmatrix} J_{t_1} \\ J_{t_2} \\ \cdot \\ \cdot \\ \cdot \\ J_{t_m} \end{bmatrix}. \tag{6}$$

In the presence of supporting contacts, we use the contact consistent Jacobian of the task,

$$J_{t|c}(q) = J_t(q)N_c(q), \tag{7}$$

as defined in [8] and the dynamically consistent null-space matrix associated with $J_c(q)$,

$$N_c(q) \triangleq I - \bar{J}_c(q)J_c(q), \tag{8}$$

established by [9].

Here, the subscript $t|c$ indicates that the task point is consistent with the contacts. The range of the Jacobian, $J_{t|c}(q)$, is the instantaneous space of task motion that is consistent with the contacts. $\bar{J}_c(q)$ is the generalized inverse [9] that ensures the dynamic consistency between the contacts and the tasks, is unique and is given by,

$$\bar{J}_c(q) = A_c^{-1}(q)J_c^T(q)\Lambda(q), \tag{9}$$

where

$$\Lambda(q) = (J_c(q)A_c^{-1}(q)J_c^T(q))^{-1}, \tag{10}$$

is the operational space kinetic energy matrix [10].

Thus, Equation (3) becomes:

$$\Phi = J_{t|c}(q)(L^T(q)C^2L(q))^{-1}J_{t|c}^T(q). \tag{11}$$

In our case, the left/right foot and the left/right hand represent the contact and the task points, respectively. The task Jacobian and the contact Jacobian can be given, respectively, by:

$$J_t(q) = \begin{bmatrix} J_{RightHand} \\ J_{LeftHand} \end{bmatrix}, J_c(q) = \begin{bmatrix} J_{RightFoot} \\ J_{LeftFoot} \end{bmatrix}. \tag{12}$$

3 Musculoskeletal Models and Experiments

3.1 Musculoskeletal Models

The musculoskeletal model used in this work is derived from upper [11] and lower [12] body models. The skeletal part of the model is represented by rigid bodies or bone segments. A reference frame is attached to each body segment and inertial parameters of the body segment are expressed in this reference frame. The upper body's kinematics contain 14 degrees-of-freedom (DOFs), which represent the shoulder, elbow, forearm, wrist, and hand. The lower body's kinematics contain 17 DOFs, which represent the hip, knee, ankle, subtalar, and metatarsophalangeal joints. The arms-torso, torso-pelvis, and pelvis-leg joints are represented by ball-and-socket joints. The remaining joints are revolute. The hip is modeled as a ball-and-socket joint, the knee is modeled as a custom joint with one DOF [13], and the foot and ankle are modeled as a custom joint with two DOFs (i.e.,

ankle dorsi-/plantar flexion, tarsal eversion/inversion). Lumbar motion is modeled as a ball-and-socket joint [14]. The shoulder is modeled as a ball-and-socket joint, the elbow is modeled with a revolute joint and the wrist is modeled with a custom joint with three DOFs (i.e., flexion/extension, ulnar/radial deviations, pronation/supination).

Muscles span the joints and generate forces and movement. Muscle line of action is defined by the origin, insertion, and via points connected to the rigid bodies. The contraction dynamics of each musculo-tendon units is modeled using a conventional Hill-type phenomenological model of muscle [15]. In our musculoskeletal model, the upper extremity, lower extremity, and back joints are actuated by 118 musculotendon actuators [12, 14]. The functional groups of muscles used in the whole-body effort characterization of pushing are given in Table 1.

The generic model was scaled based on the measurement-based scaling [16] to match subjects anthropometry based on experimentally measured markers placed on anatomical landmarks. A virtual marker set is placed on the unscaled model based on these anatomical landmarks. The scale factors for a body segment are determined by comparing distance measurements between the virtual markers and the corresponding experimental marker positions. The marker locations are obtained using motion capture equipment. Before each motion capture experiment, a static trial is performed on the subject to assist scaling the musculoskeletal model (for example, with markers attached to the medial and lateral femoral epicondyles and medial and lateral malleoli). Then, each body segment of the model is scaled by measuring the positions of two experimental markers on that body segment on the subject, and the size of the body segment is uniformly adjusted so the virtual markers are co-located with the experimental markers. The mass of the model is scaled by proportionally adjusting the mass of each body segment so the total mass of the model equals the measured mass of the subject.

3.2 Experiments

Motion capture experiments were conducted on a healthy man pushing against a heavy object. The subject was instructed to push against the object with the highest possible force he could exert in a horizontal direction. After each pushing trial, the subject was asked to change his posture in order to push the object more comfortably. This was repeated for seven different configurations. The subject's motion was captured at $100\,Hz$ using an eight-camera Motion Analysis [17] motion capture system. The ground reaction forces were captured at $4000\,Hz$ with two Bertec force plates [18]. The pushing force was measured from the force sensors [19] placed between the object and the hands of the subject.

Table 1. Functional Groups of Muscles [12, 14, 16] Used in the Whole-Body Muscular Effort Analysis

Shoulder Adduction	Shoulder Abduction
Coracobrachialis	Deltoid
Infraspinatus	Subscapularis
Latissimus dorsi	Trapezius
Pectoralis major	
Teres major	
Scapular Retraction	**Scapular Elevation/Depression**
Trapezius	Levator scapulae
	Latissimus dorsi
	Trapezius
Arm Flexion	**Arm Extension**
Biceps brachii	Latissimus dorsi
Coracobrachialis	Teres major
Pectoralis major	Triceps minor
Hip Adduction	**Hip Abduction**
Adductor magnus	Gluteus medius
Hip Flexion	**Hip Extension**
Gluteus medius	Adductor magnus
	Biceps femoris
	Gluteus maximus
	Semimembranosus
Knee Flexion	**Knee Extension**
Biceps femoris	Vasti
Semimembranosus	Rectus Femoris
Ankle Dorsi-/Plantar Flexion	**Ankle Eversion/Inversion**
Extensor digitorum	Extensor digitorum
Extensor hallucis	Peroneus brevis
Peroneus tertius	Peroneus longus
Tibialis anterior/posterior	Peroneus tertius
Flexor digitorum	Extensor hallucis
Flexor hallucis	Flexor digitorum
Gastrocnemius	Flexor hallucis
Peroneus brevis/longus	Tibialis anterior
Soleus	Tibialis posterior
Trunk Flexion/Extension/Rotation	
External oblique	
Internal oblique	
Erector spinae	

4 Musculoskeletal Simulations and Results

4.1 Belted Ellipsoid Representation of Effort Function

Robotics brought efficient algorithms and tools for the analysis and control of multi-degree of freedom redundant manipulators. The belted ellipsoid established by the author [20] is a geometric representation that characterizes the inertial properties perceived at a given position and an orientation of an end effector. Ellipsoid representations only provide a description of the square roots of effective mass (inertia) in (or about) a direction. A belted ellipsoid is defined as a geometric representation that characterizes the actual magnitude of these properties. A point on the ellipsoid represented by a vector v is transformed into a point on the belted ellipsoid represented by a vector w, where the vector w is collinear to v and is of magnitude equal to $v^T v$ [20].

In robotics, the belted ellipsoid representation [20] is used to assess the performance of a multi-degree of freedom manipulator by describing its effective mass along a desired direction of the end-effector motion. In illustrating human muscular effort geometrically, the belted ellipsoid representation can be used to efficiently describe the actual value of the effort along a desired direction. This information provides an understanding of the muscular effort required to position the body or to perform a desired task.

4.2 Musculoskeletal Simulations

Fig. 3 shows the three-dimensional simulations of two extreme postures and five intermediate postures of the subject while pushing an object. Fig. 4 illustrates two different postures used while pushing the object. The ground contact forces, F_c, shown with green arrows, are measured from the force plates and used for the calculation of the muscular effort. In Figure 4, the musculoskeletal simulation of pushing while adopting an unnatural posture is shown in the left image with the belted ellipsoid (blue) of whole-body muscular effort reflected at both hands. The measured force at the contact point from the force sensor is $50.4\,N$ in total for the left and right hands. The red arrow depicts the direction of the applied force, F, aligned with the maximum semi-axis of the belted ellipsoid. This shows that the whole-body effort is maximized in the pushing direction. The right image in Fig. 4 shows the musculoskeletal simulation of pushing while adopting a natural posture with the belted ellipsoid (blue) of whole-body muscular effort reflected at both hands. The measured force at the contact point from the force sensor is $379\,N$ in total for the left and right hands. The red arrow depicts the direction of the applied force, F, aligned with the minimum semi-axis of the belted ellipsoid. This shows that the whole-body effort is minimized in the pushing direction. Between the two pushing postures, there is a 146 times reduction in muscular effort in the direction of pushing (i.e. task).

Fig. 5(a) illustrates the change in whole-body effort of pushing versus the total pushing force (i.e., summation of horizontal forces applied from the left and right hands) measured from the force sensors and force plates, for seven

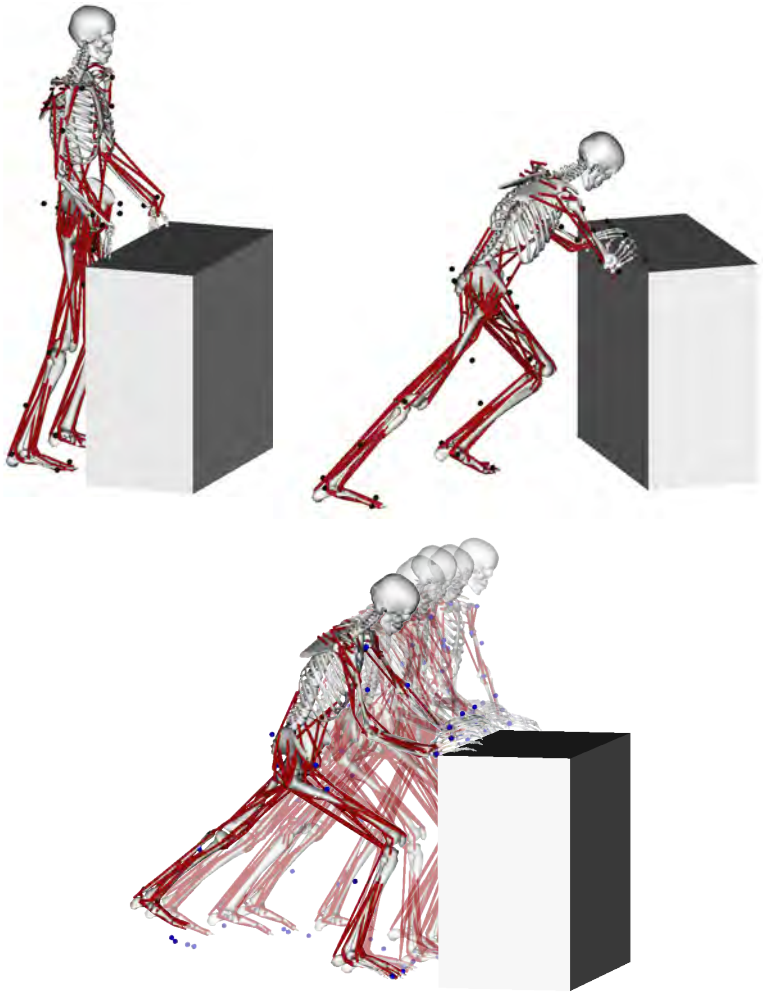

Fig. 3. Three-dimensional simulations of (top) two extreme postures (i.e., the most and the least effort), and (bottom) intermediate postures (i.e., decreasing effort from the right to the left postures) while pushing an object. Motion capture and force plate data were collected with a healthy male subject pushing against an object and the scaled full-body model was used to generate the pushing simulations.

different configurations. Figure 5(b) illustrates the total pushing force versus the pushing configuration. The total force of pushing is $50.4\,N$, $82.6\,N$, $106\,N$, $111\,N$, $121\,N$, $239.6\,N$, and $379\,N$ for the configurations from one (i.e., most effort) to seven (i.e., least effort).

As more comfortable postures were adopted, the muscular effort decreased significantly with maximum reduction of 146, while the maximum force exerted

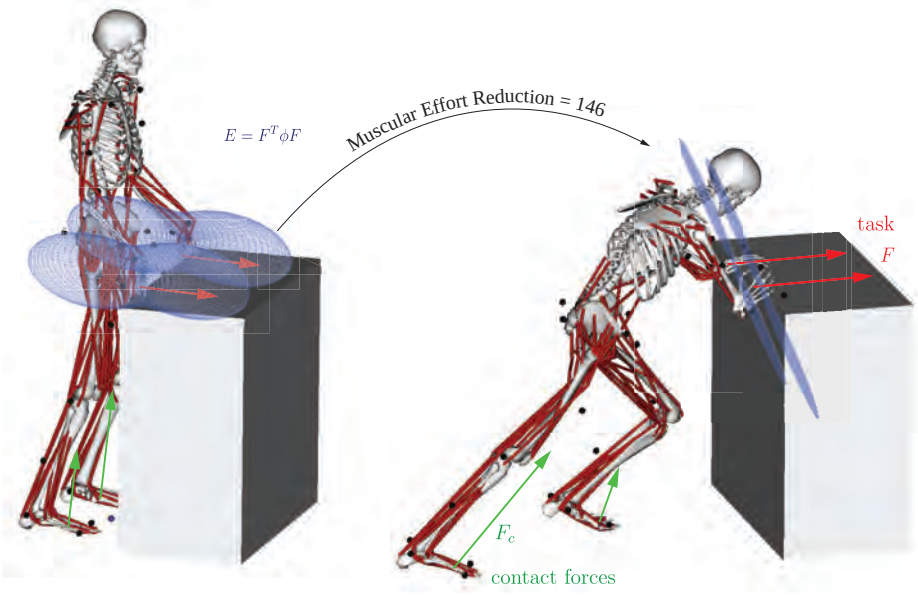

Fig. 4. Whole-body effort during pushing: The musculoskeletal simulations of pushing while adopting the least (left) and the most (right) comfortable pushing postures. The belted ellipsoid [20] (blue) of whole-body muscular effort is given with the directions of the task forces (red arrows), F, and the ground reaction forces (green arrows), F_c.

on the object increased from 82.6 N to 239.6 N at intermediate postures to reach its maximum, 379 N, for the posture with the least effort production.

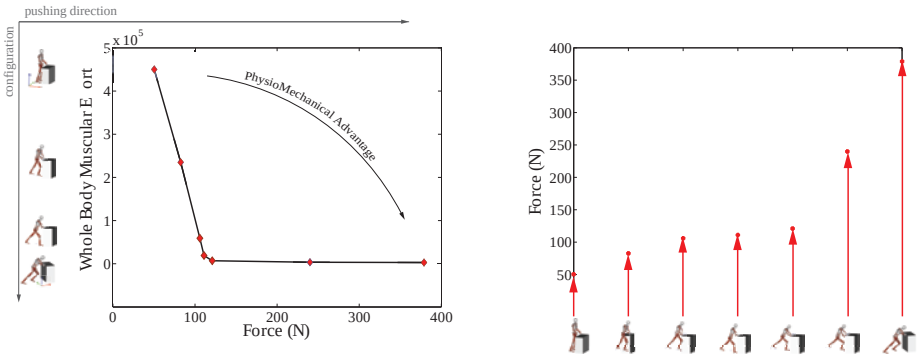

Fig. 5. (a) Whole-body muscular effort versus the pushing force. (b) Total pushing force versus the pushing configuration.

5 Conclusion

A strategy that employs physiomechanical advantage to produce a posture and task force corresponds to a minimization of muscular effort. The whole-body muscle effort criterion was implemented to analyze several pushing postures. While in static poses, the muscles produce joint torques to act against the gravitational torques, in dynamic skills, inertial forces are part of the effort and are taken into account accordingly. In order to achieve dynamic consistency between the task and the contacts, the contact consistent Jacobian of the task was calculated and was included in the computation of the whole-body muscular effort. The results of the analysis showed that as the subject adopted more comfortable postures to push against an object, the transmission from the ground reaction forces and the weight of the subject to the resulting force increased significantly. This optimal transmission resulted in a whole-body effort reduction of 146, benefiting from the skeletal configuration as well as from the muscle kinematics. The minimization of the whole-body effort is a criterion associated with natural human motion and can be used to contitute the desired musculoskeletal posture to be achieved by the controller. Our approach for the characterization of human muscular effort involves scaling a musculoskeletal model to match an individual's anthropometry. It provides subject-specific muscle and joint parameters, such as musculotendon lengths, moment arms, lines of action, and joint topology. As such, this technique inherently accounts for differences between individuals stemming from differences in body size. The technique would, therefore, predict that subjects of different stature would perform the same task (i.e., pushing with maximum force) with slightly different joint kinematics.

Acknowledgments. The authors thank Jessica Rose, Kristine Bruce and Gerald Brantner for their help with the motion capture experiments. The data collection was done at Lucile Packard Children Gait Hospital at Stanford University. This work was supported by the Global Creative Leaders (GCL) program of the University of Tokyo Graduate School of Engineering.

References

1. Hermens, F., Gielen, S.: Posture-based or trajectory-based movement planning: a comparison of direct and indirect pointing movements. Experimental Brain Research. 159(3), 304-348 (2004)
2. Vetter, P., Flash, T., Wolpert, D.M.: Planning movements in a simple redundant task. Current Biology. 12(6), 488-491 (2002)
3. DeSapio, V., Warren, J., Khatib, O.: Predicting reaching postures using a kinematically constrained shoulder model. In: Proceedings of the Tenth International Symposium Advances in Robot Kinematics, pp. 209-218. Heidelberg, Germany (2006)
4. Khatib, O., Warren, J., DeSapio, V., Sentis, L.: Human-like motion from physiologically-based potential energies. In: J. Lenarčič and C. Galletti (Eds.) On Advances in Robot Kinematics. pp. 149-163 (2004)

5. Thelen, D.G., Anderson, F.C., Delp, S.L.: Generating dynamic simulations of movement using computed muscle control. Journal of Biomechanics. 36, 321-32 (2003)
6. Khatib, O., Demircan, E., DeSapio, V., Sentis, L. Besier, T., Delp, S.: Robotics-based Synthesis of Human Motion. Journal of Physiology Paris. 103(3-5), 211-219 (2009)
7. Lieber, R., L.: Skeletal Muscle Structure, Function, and Plasticity. Second Edition. Lippincott Williams and Wilkins (Publisher) (2002)
8. Park, J., Khatib, O.: Multi-link multi-vontact force control for manipulators. In: IEEE Int. Conf. on Robotics and Automation, pp. 3613–3618 (2005)
9. Khatib, O.: Motion/Force Redundancy of Manipulators. In: Proceedings of the Japan-USA Symposium on Flexible Automation, pp. 337-342, Kyoto, Japan, July (1990)
10. Khatib, O.: A unified approach for motion and force control of robot manipulators: The operational space formulation. International Journal of Robotics and Automation. 3(1):43-53 (1987)
11. Holzbaur, K.R., Murray, W.M., Delp, S.L.: A model of the upper extremity for simulating musculoskeletal surgery and analyzing neuromuscular control. Experimental Brain Research. 33(6), 829-840 (2005)
12. Delp, S.L., Loan, P., Hoy, M.G., Zajac, F.E., Topp, E.L., Rosen, J.M.: An interactive graphics-based model of the lower extremity to study orthopaedic surgical procedures. IEEE Transactions on Biomedical Engineering. 37(8), 757-767 (1990)
13. Seth, A., Sherman, M., Eastman, P., Delp, S.L.: Minimal formulation of joint motion for biomechanisms. Nonlinear Dynamics. 62(1), 291-303 (2010)
14. Anderson, F.C., Pandy, M.G.: A dynamic optimization solution for vertical jumping in three dimensions. Comput.Meth.Biomech.Biomed.Eng. 2(3), 201-231 (1999)
15. Hill, A. V.: The heat of shortening and dynamics constants of muscles. Proc. R. Soc. Lond. B (London: Royal Society), 126(843):136195 (1938)
16. Delp, S.L., Anderson, F.C., Arnold, A.S., Loan, P., Habib, A., John, C.T., Guendelman, E., Thelen, D.G.: OpenSim: Open-source software to create and analyze dynamic simulations of movement. IEEE Transactions on Biomedical Engineering. 55, 1940-1950 (2007)
17. Motion Analysis, Santa Rosa, CA, USA, http://motionanalysis.com/
18. Bertec, Columbus, OH, USA, http://bertec.com/
19. Tekscan Inc., South Boston, MA, USA, http://www.tekscan.com/flexible-force-sensors/
20. Khatib, O.: Inertial properties in robotics manipulation: An object-level framework. The International Journal of Robotics Research. 14(1), 19-36 (1995)